blood®
Regular Article

MYELOID NEOPLASIA

Myeloid lncRNA *LOUP* mediates opposing regulatory effects of RUNX1 and RUNX1-ETO in t(8;21) AML

Bon Q. Trinh,[1] Simone Ummarino,[1] Yanzhou Zhang,[1] Alexander K. Ebralidze,[1] Mahmoud A. Bassal,[2,3] Tuan M. Nguyen,[1,4] Gerwin Heller,[5] Rory Coffey,[1] Danielle E. Tenen,[6] Emiel van der Kouwe,[7] Emiliano Fabiani,[8,9] Carmelo Gurnari,[8] Chan-Shuo Wu,[3] Vladimir Espinosa Angarica,[3] Henry Yang,[3] Sisi Chen,[1] Hong Zhang,[1] Abby R. Thurm,[2,10] Francisco Marchi,[2,11] Elena Levantini,[1,2,12] Philipp B. Staber,[7] Pu Zhang,[1] Maria Teresa Voso,[8] Pier Paolo Pandolfi,[13] Susumu S. Kobayashi,[1,2,14] Li Chai,[2,15] Annalisa Di Ruscio,[1,16,17] and Daniel G. Tenen[1,10]

[1]Harvard Medical School Initiative for RNA Medicine, Harvard Medical School, Boston, MA; [2]Harvard Stem Cell Institute, Harvard University, Boston, MA; [3]Cancer Science Institute of Singapore, National University of Singapore, Singapore; [4]Chemical Biology and Therapeutics Science, Broad Institute of MIT and Harvard, Cambridge, MA; [5]Division of Oncology, Department of Medicine I, Medical University of Vienna, Vienna, Austria; [6]Division of Endocrinology, Diabetes, and Metabolism, Beth Israel Deaconess Medical Center, Harvard Medical School, Boston, MA; [7]Division of Hematology, Department of Medicine I, Medical University of Vienna, Vienna, Austria; [8]Department of Biomedicine and Prevention, University of Rome Tor Vergata, Rome, Italy; [9]Saint Camillus International University of Health Sciences, Rome, Italy; [10]Stanford University School of Medicine, Stanford, CA; [11]University of Florida, Gainesville, FL; [12]Institute of Biomedical Technologies, National Research Council (CNR), Area della Ricerca di Pisa, Pisa, Italy; [13]Department of Pathology, Beth Israel Deaconess Cancer Center, Harvard Medical School Boston, MA; [14]Division of Translational Genomics, Exploratory Oncology Research and Clinical Trial Center, National Cancer Center, Kashiwa, Chiba, Japan; [15]Department of Pathology, Brigham and Women's Hospital, Harvard Medical School, Boston, MA; [16]Cancer Research Institute, Beth Israel Deaconess Medical Center, Boston, MA; and [17]Department of Translational Medicine, University of Eastern Piedmont, Novara, Italy

KEY POINTS

- **lncRNA *LOUP* coordinates with RUNX1 to induce *PU.1* long-range transcription, conferring myeloid differentiation and inhibiting cell growth.**
- **RUNX1-ETO limits chromatin accessibility at the *LOUP* locus, causing inhibition of *LOUP* and *PU.1* expression in t(8;21) AML.**

The mechanism underlying cell type-specific gene induction conferred by ubiquitous transcription factors as well as disruptions caused by their chimeric derivatives in leukemia is not well understood. Here, we investigate whether RNAs coordinate with transcription factors to drive myeloid gene transcription. In an integrated genome-wide approach surveying for gene loci exhibiting concurrent RNA and DNA interactions with the broadly expressed Runt-related transcription factor 1 (RUNX1), we identified the long noncoding RNA (lncRNA) originating from the upstream regulatory element of *PU.1* (*LOUP*). This myeloid-specific and polyadenylated lncRNA induces myeloid differentiation and inhibits cell growth, acting as a transcriptional inducer of the myeloid master regulator *PU.1*. Mechanistically, *LOUP* recruits RUNX1 to both the *PU.1* enhancer and the promoter, leading to the formation of an active chromatin loop. In t(8;21) acute myeloid leukemia (AML), wherein RUNX1 is fused to ETO, the resulting oncogenic fusion protein, RUNX1-ETO, limits chromatin accessibility at the *LOUP* locus, causing inhibition of *LOUP* and *PU.1* expression. These findings highlight the important role of the interplay between cell-type–specific RNAs and transcription factors, as well as their oncogenic derivatives in modulating lineage-gene activation and raise the possibility that RNA regulators of transcription factors represent alternative targets for therapeutic development.

Introduction

Lineage-control genes that dictate cellular identities are often expressed in dynamic and hierarchical patterns.[1-3] Disturbance of these established normal patterns results in anomalies.[4] In the blood system, the ETS-family transcription factor PU.1 (also known as Spi-1) is essential for myeloid differentiation. *PU.1* is silent in most tissues and cell types but is expressed at the highest levels in myeloid cells including granulocytes and monocytes.[5] Downregulation of *PU.1* impairs myeloid cell differentiation, leading to acute myeloid leukemia (AML).[6,7] *PU.1* is a major downstream transcriptional target of Runt-related transcription factor 1 (RUNX1), which is expressed in many different cell types and plays diverse biological roles in hematopoiesis, and development of neurons, hair follicles, and skin.[8-12] In AML with the t(8;21) chromosomal translocation, a portion of *RUNX1* containing the Runt DNA-binding domain is fused to *ETO*, giving rise to the oncogenic transcription factor fusion RUNX1-ETO.[13,14] Previously, we have reported that RUNX1-ETO inhibits *PU.1* expression[15] but the mechanism underlying this transcriptional inhibition remains to be determined. In general, how broadly expressed transcription factors, such as RUNX1, modulate cell type- and gene-specific induction and how their chimeric derivatives disrupt this normal regulation in leukemia are poorly understood.

Transcription of many cell type-specific genes is induced by enhancer elements, which are located at variable distances from

gene targets.[16,17] For instance, *PU.1* transcription is induced by the formation of a specific chromatin loop resulting from the interaction between the upstream regulatory element (URE; −17 kb in humans and −14 kb in mice) and the proximal promoter region (PrPr).[18-20] Interestingly, abrogation of RUNX1-binding motifs at the URE reduces URE-PrPr interaction, resulting in decreased *PU.1* expression in myeloid cells.[8,15] Because RUNX1 is broadly expressed, how this transcription factor modulates chromatin structure in such a gene- and cell type-specific manner remains unclear.

With advances in whole-transcriptome sequencing over the last decade, thousands of noncoding RNAs (ncRNAs) have been unveiled.[21] Arbitrarily defined as ncRNAs of at least 200 nucleotides in length, long noncoding RNAs (lncRNAs) are implicated in displaying tissue-specific expression patterns[22,23] and might undergo posttranscriptional processing such as splicing and polyadenylation.[24] Through interactions with DNAs, proteins, and other RNAs, lncRNAs regulate fundamental cellular processes including transcription, RNA stability, and DNA methylation.[24-26] To date, only a few lncRNAs have been precisely mapped and functionally defined,[23] leaving most lncRNAs poorly annotated and largely unexplored.

In this study, we identified a myeloid-specific lncRNA, termed "long noncoding RNA originating from the URE of *PU.1*," or *LOUP*, from an integrated genome-wide approach aimed at screening for gene loci exhibiting concurrent RNA and DNA interactions with RUNX1. We demonstrated that *LOUP* induces *PU.1* expression, conferring myeloid differentiation, and inhibiting cell growth. *LOUP* serves as a central hub in opposing regulation by RUNX1 and its derived oncogenic fusion, RUNX1-ETO. Our findings provide a model explaining how a lineage gene is activated in normal myeloid development and dysregulated in leukemia.

Methods

Cell lines and cell culture

U937, HL-60, K562, HEK293T, RAW 264.7, NB4, Jurkat, Kasumi-1, and THP-1 cells were obtained from the American Type Culture Collection (ATCC). U937, HL-60, NB4, Jurkat, and K562 cells were cultured in full RPMI 1640 medium (supplemented with 10% [v/v] fetal bovine serum [FBS; Cellgro] and 1% penicillin-streptomycin). Kasumi-1 cells were cultured in the same medium plus 20% (v/v) FBS. THP-1 cells were cultured in full RPMI 1640 medium supplemented with 2-mercaptoethanol to a final concentration of 0.05 mM. HEK293T and RAW 264.7 cells were cultured in Dulbecco modified Eagle medium supplemented with 10% (v/v) FBS and 1% penicillin-streptomycin. All cells were grown at 37°C in 5% (v/v) CO_2 and humidified incubators.

AML patient sample collection

Bone marrow (BM) samples were obtained from newly diagnosed patients with AML at the Tor Vergata University Hospital (Rome, Italy) with informed consent. Diagnoses were performed according to the 2016 revision to the World Health Organization classification of myeloid neoplasms and acute leukemia.[27] BM mononuclear cells were isolated by Ficoll gradient centrifugation using Lympholyte-H (Cedarlane), according to the manufacturer's instructions.

Methods for assaying myeloid culture of primary cells; interactions of RNA, DNA, and protein with chromatin; chromatin structure; gene-expression manipulation; and bioinformatic analyses are in supplemental Methods (available on the *Blood* Web site).

Results

Identification of RUNX1-interacting RNAs at myeloid gene loci

We started out by performing a transcriptome-wide survey for RUNX1-interacting RNAs in the monocytic cell line THP-1 using formaldehyde RNA immunoprecipitation (RIP) sequencing (RIP-seq).[28,29] RUNX1-interacting RNAs were captured by anti-RUNX1 antibody (supplemental Figure 1A-C) and sequenced by paired-end massively parallel sequencing. By annotating 10 109 high-confident RUNX1-RIP peaks to the GRCh38.p12 gene catalog,[30] we identified 6035 gene loci carrying ≥1 of these peaks (supplemental Figure 1D, left). Most of the peaks were detected within transcript bodies and promoters (supplemental Figure 1E). To identify genes exhibiting concurrent RUNX1-RNA and RUNX1-DNA interactions, we annotated 24 185 high-confidence RUNX1-chromatin immunoprecipitation (ChIP) peaks to the same gene catalog and identified 13 275 corresponding gene loci (supplemental Figure 1D, right). The majority of these peaks were found at intronic, promoter, and intergenic regions (supplemental Figure 1F). Because most RUNX1-RIP and RUNX1-ChIP peaks were distributed at coding gene loci (Figure 1A-B), we focused our analyses on this gene group. By intersecting these genes with a list of 78 myeloid genes defined by their known roles in myeloid development, or as myeloid molecular markers (supplemental Table 1), we obtained 15 myeloid gene loci displaying both RUNX1-RIP and RUNX1-ChIP peaks (Figure 1C; supplemental Table 2). *PU.1*, a master regulator of myeloid development and a well-known transcriptional target of RUNX1,[8] was among these genes. Intriguingly, we observed RNA peaks at the upstream region of *PU.1* (Figure 1D). We further validated this observation by RUNX1 RIP-quantitative polymerase chain reaction (qPCR) (Figure 1E). Additional myeloid genes showing RUNX1-RIP peaks and RUNX1-ChIP peaks are presented in supplemental Figure 1G. The presence of previously uncharacterized RNAs, arising from the upstream region of the *PU.1* locus, and able to interact with RUNX1, suggests their potential role in controlling *PU.1* expression through RUNX1-mediated transcriptional regulation.

Characterization of the RUNX1-interacting lncRNA *LOUP*

To map the RUNX1-interacting transcript(s), we inspected the RNA expression and epigenetic landscape at the upstream region of the *PU.1* locus (Figure 2A). Remarkably, the RNA-sequencing (RNA-seq) track view revealed 2 distinct RNA peaks. A narrow peak was observed at the URE, which corresponded to an area of open chromatin in myeloid cells as indicated by strong DNase I hypersensitivity signals (Figure 2A, DNase-seq [or DNase sequencing]). This element was also enriched with histone post-translational modifications such as H3K27ac, H3K4me1, and H3K4me3 (Figure 2A, ChIP-seq [or ChIP sequencing]), which are typical features of active enhancers.[31,32] A broad peak was proximal to the promoter region. Notably, these peaks were present in myeloid cell lines (THP-1 and HL-60) and primary monocytes, but not in the lymphoid cell line Jurkat, which does not express *PU.1*

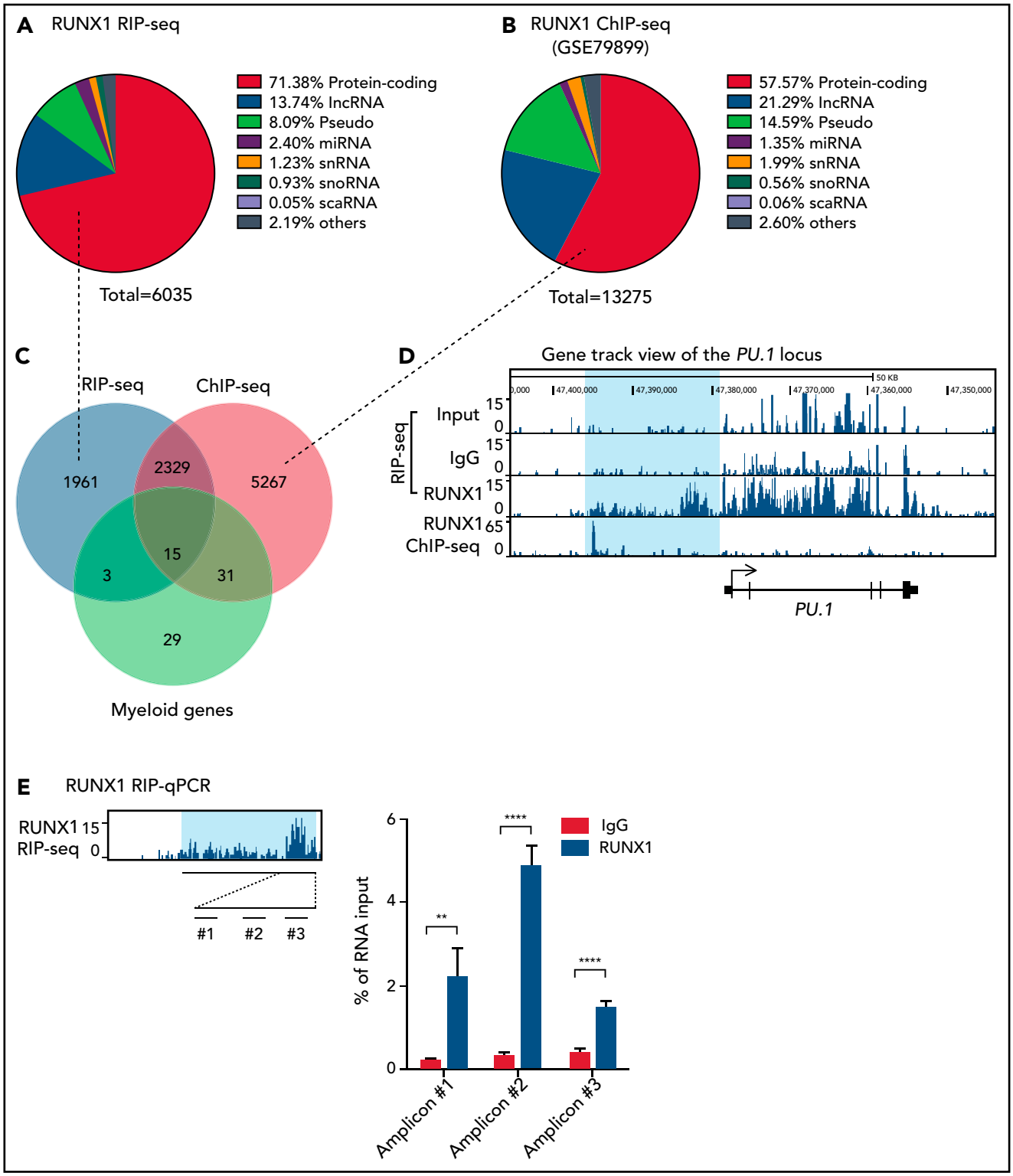

Figure 1. Screening of gene loci exhibiting concurrent RUNX1 RNA and DNA interactions in THP-1 cells. (A-B) Pie charts showing proportions of RUNX1 RIP-seq peaks and RUNX1 ChIP-seq peaks in coding and noncoding gene families. ChIP-seq data were from published source[53] under the Gene Expression Omnibus (GEO) accession number GSE79899; snoRNA, small nucleolar RNAs; snRNA, small nuclear RNA; miRNA, microRNA; scaRNA, small cajal body-specific RNA. (C) Venn diagram intersecting RUNX1 RIP-seq and RUNX1 ChIP-seq gene lists and the myeloid gene list. (D) Gene track view of the *PU.1* locus including the upstream region (highlighted in blue). Shown are RIP-seq tracks (Input, IgG, and RUNX1) and RUNX1 ChIP-seq tracks (GSM2108052). Data were integrated in the University of California, Santa Cruz (UCSC) genome browser. (E) RUNX1 RIP-qPCR confirmation. Left panel: location of 3 PCR amplicons (#1, #2, #3). Right panel: enrichment of RNAs captured by anti-RUNX1 antibody and IgG control at 3 amplicons relative to input. Error bars indicate SD (n = 3). $^{**}P < .01$; $^{****}P < .0001$. See also supplemental Figure 1 and supplemental Table 3.

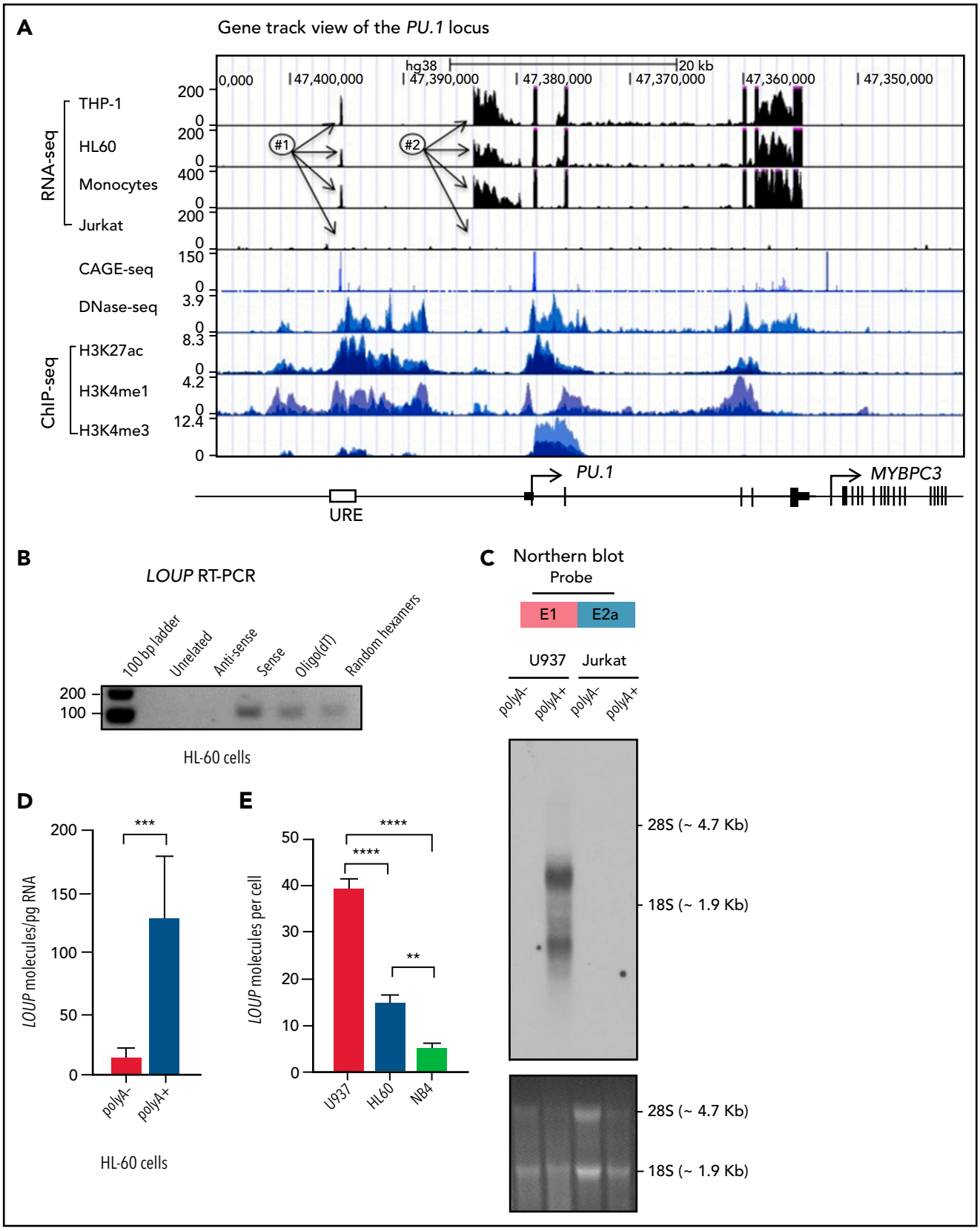

Figure 2. Characterization of long noncoding RNA *LOUP*. (A) Gene track view of the genomic region encompassing the *PU.1* locus. RNA-seq tracks include THP-1, HL60, primary monocytes, and Jurkat. DNase-seq and ChIP-seq are overlay tracks of monocyte and myeloid cell lines. These data were processed from published data in GEO (see "Methods" for details). The CAGE-seq track was imported from the FANTOM5 project; #1, #2, and arrows point to locations of the RNA peaks. (B) RT-PCR analysis of *LOUP*'s transcript features. First-strand cDNAs were generated from HL-60 total RNA using a primer that does not anneal to the *PU.1* locus (Unrelated), random hexamers, Oligo(dT), and strand-specific primers (antisense and sense). (C) Northern blot analysis of *LOUP*. polyA$^-$ and polyA$^+$ RNA fractions were isolated from U937 and Jurkat cells.

messenger RNA (mRNA), indicating a cell-type–specific expression pattern. Reverse transcription polymerase chain reaction (RT-PCR) and Sanger sequencing analysis identified exon junctions connecting these 2 peaks in both human and murine cell lines (supplemental Figure 2A). Strand-specific RT-PCR analysis confirmed that the transcript is sense with respect to the *PU.1* gene (Figure 2B). A strong Cap-analysis gene-expression sequencing (CAGE-seq) peak is present within the URE and in the sense genomic orientation (Figure 2A CAGE-seq), suggesting the presence of the 5′ end of a transcript. We further identified this 5′ end including a transcription start site (TSS) of the RNA within the homology region 1 (H1) of the URE[18] (supplemental Figure 2B-C). Although a splicing event was detected within the second exon, intron retention was dominant as shown by the presence of a ~2.3 kb major transcript and a ~1.0 kb minor transcript (Figure 2C-D). The transcripts were detectable in the myeloid cell line U937, but not in the lymphoid cell line Jurkat, further indicating their cell-type specificity (Figure 2C). Notably, the RNA exhibited very low coding potential similar to that of other known lncRNAs (supplemental Figure 2E) as assessed by PhyloCSF software.[33] Additionally, no known protein domains were found (data not shown) using PFAM software.[34] Thus, we named the RNA transcript "long noncoding RNA originating from the URE of *PU.1*", or *LOUP*. A *LOUP* homolog is also expressed and originated from the URE in murine cells (Ensembl ID #ENSMUST00000131400). Quantitative RT-PCR (qRT-PCR) analyses of subcellular fractionations revealed that it resides in both the cytoplasm and the nucleoplasm compartments, and was particularly enriched in the chromatin fraction (supplemental Figure 2F). The lncRNA is polyadenylated, being detected from oligo(dT)-primed complementary DNAs (cDNAs) (Figure 2B) and enriched in the polyA$^+$ RNA fraction (Figure 2C-D; supplemental Figure 2G). *LOUP* is a low-abundant lncRNA; the spliced form is expressed as ~40, 14, and 5 copies per cell in U937, HL-60, and NB4, respectively (Figure 2E). The lncRNA was barely detectable as its premature (nonspliced) form in total RNA as well as in the nuclear RNA fraction (supplemental Figure 2H-I). Altogether, these findings established *LOUP* as a polyadenylated lncRNA that emanates from the URE and extends toward the PrPr.

LOUP is a myeloid-specific lncRNA that is coexpressed with myeloid-lineage gene *PU.1*

We sought to explore *LOUP* expression in normal tissues and cell types. By examining the *LOUP* transcript profile in different human tissue types from the Illumina Body Map data set, we noticed that this lncRNA was barely detectable in most tissues but was elevated in leukocytes (Figure 3A). Remarkably, comparing with 2 of its closest neighbor genes, *PU.1* and *SLC39A13* (supplemental Figure 2D), the *LOUP* expression pattern was similar to that of *PU.1* mRNA (Figure 3A-B) but not of *SLC39A13* (supplemental Figure 3A). Additionally, *LOUP* transcript levels were not correlated with those of its interacting partner, *RUNX1* (supplemental Figure 3B). To further delineate the relationship between *LOUP* and *PU.1* transcript levels and lineage identity in individual blood cells, we used single-cell RNA (scRNA)-sequencing (scRNA-seq) analyses (supplemental Figure 3C). Notably, *LOUP* and *PU.1* were both enriched in myeloid cells, comprising monocytes, macrophages, and granulocytes (supplemental Figure 3D-G). Expectedly, *RUNX1* was broadly expressed in myeloid cells as well as lymphoid cells (T, B, and natural killer [NK]) (supplemental Figure 3H). By stratifying the mononuclear cell population into *LOUP*$^+$/*PU.1*$^+$ and *LOUP*$^-$/*PU.1*$^-$ groups based on *LOUP* and *PU.1* expression levels, we noted that *LOUP*$^-$/*PU.1*$^-$ cells were associated with T, B, and NK cells. Remarkably, 99.3% of *LOUP*$^+$/*PU.1*$^+$ cells were linked to the myeloid identity (Figure 3C). Consistent with this observation, top biological processes associated with expression of *LOUP* and *PU.1* were monocyte, macrophage, and granulocyte functions (supplemental Figure 3I; supplemental Table 4). We further examined expression patterns of *LOUP* and *PU.1* during myeloid differentiation. qRT-PCR analyses of purified murine hematopoietic cell populations showed low *Loup* levels in long-term hematopoietic stem cells (LT-HSCs), short-term hematopoietic stem cells (ST-HSCs), common myeloid progenitors (CMPs), and megakaryocyte-erythroid progenitors (MEPs). Remarkably, *Loup* expression was elevated in myeloid progenitor cells (granulocyte-macrophage progenitors [GMPs]) and was highest in definitive myeloid cells (Figure 3D). A similar expression pattern was seen with *PU.1* (Figure 3E). Taken together, our data indicated that *LOUP* and *PU.1* transcript levels were associated with the myeloid identity.

LOUP induces *PU.1* expression, promotes myeloid differentiation, and inhibits cell growth

To test our hypothesis that *LOUP* induces *PU.1* expression, we first investigated the impact of loss-of-function of *LOUP* on *PU.1* expression. Depletion of *LOUP* in macrophage cell line U937, which expresses a high level of *LOUP* (Figure 2E), via clustered regularly interspaced short palindromic repeats (CRISPR)/CRISPR-associated protein 9 (Cas9) technology, resulted in a significant reduction in *PU.1* mRNA levels (Figure 4A; supplemental Figure 4A-E). In line with this finding, knockdown of *LOUP* by short hairpin RNAs (shRNAs) in CD34$^+$ hematopoietic stem/progenitor cells (HSPCs) cultured with myeloid differentiation-promoting cytokines, including interleukin 3 (IL-3), granulocyte-macrophage colony-stimulating factor (GM-CSF), and granulocyte colony-stimulating factor (G-CSF), resulted in *PU.1* reduction (Figure 4B). In gain-of-function experiments, in *trans*-overexpression of *LOUP* resulted in significant induction of *PU.1* (supplemental Figure 4F-G). Remarkably, in *cis* locus-specific induction of endogenous *LOUP* via the CRISPR/dCas9-VP64 activation system yielded a comparable increase in *PU.1* expression (Figure 4C; supplemental Figure 4A). *LOUP* overexpression was associated with a decrease in total cell number (Figure 4D), whereas *LOUP* depletion was associated with increased cell proliferation (supplemental Figure 4H), suggesting that *LOUP* inhibits cell growth. Consistent with the important role of *PU.1* in myeloid differentiation,[6,35,36] *LOUP* depletion by either shRNAs or CRISPR/Cas9 technology was associated with a reduction in expression of the myeloid marker CD11b (Figure 4E; supplemental Figure 4I), whereas *LOUP* overexpression resulted in an increase in CD11b levels

Figure 2 (continued) Top panel: schematic of the probe location spanning exon junction (E1 and E2a; see supplemental Figure 2D). Middle panel: northern blot detection of *LOUP*'s major and minor transcripts. Bottom panel: RNA gel demonstrating relative migration between 28S and 18S rRNAs stained with ethidium bromide. (D) qRT-PCR analysis of *LOUP* levels in polyA$^-$ and polyA$^+$ RNA fractions isolated from HL-60 cells. Error bars indicate SD (n = 3). ***$P < .001$. (E) Calculation of *LOUP* transcript per cell by qRT-PCR. The *LOUP* RNA standard curve was generated by in vitro transcription. Error bars indicate SD (n = 3). **$P < .01$; ****$P < .0001$. See also supplemental Figure 2 and supplemental Table 3.

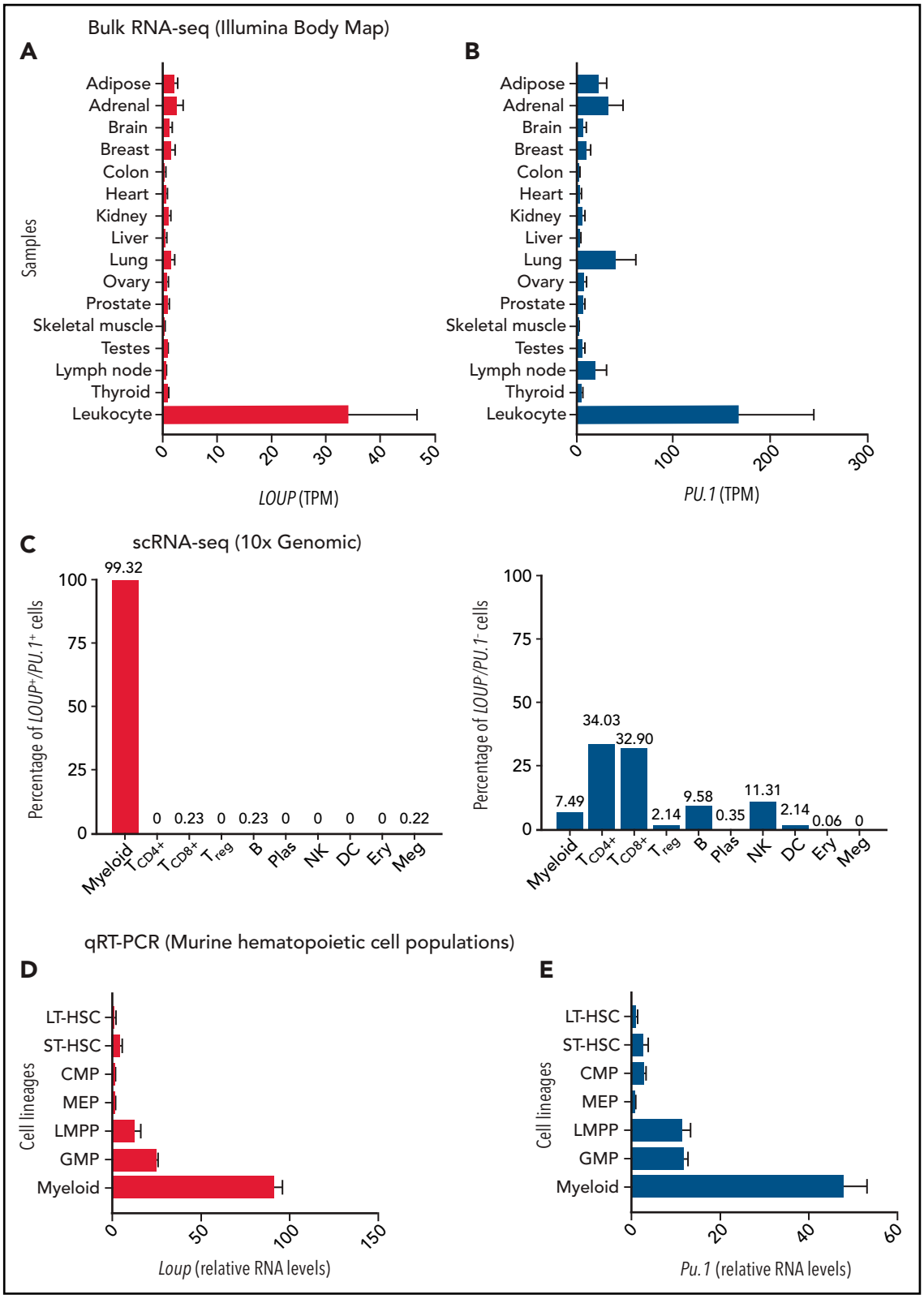

Figure 3. Expression profiles of *LOUP* and *PU.1* in normal tissues and cell lineages. (A-B) Transcript profiles of *LOUP* and *PU.1* in human tissues. Shown are transcript counts from the Illumina Body Map RNA-seq data set (ArrayExpress [AE]: E-MTAB-513). Error bars indicate SD (n = 2). (C) The proportion of cell lineages corresponding to transcript levels of *LOUP* and *PU.1*. scRNA-seq data of human mononuclear cells were retrieved from the 10x Genomic Project.[54] Myeloid includes monocytes, macrophages, and granulocytes. Numbers on each bar indicate the percentage of each cell type within $LOUP^{+}/PU.1^{+}$ (left panel) and $LOUP^{-}/PU.1^{-}$ groups (right panel), respectively. (D-E) qRT-PCR analysis of *Loup* RNA and *Pu.1* mRNA levels in murine hematopoietic stem, progenitor, and mature (myeloid) cell populations. Data are shown relative to LT-HSCs. Error bars indicate SD (n = 2). See also supplemental Figure 3 and supplemental Table 3. B, B lymphocyte; CMP, common myeloid progenitor; DC, dendritic cell; Ery, erythrocyte; GMP, granulocyte-macrophage progenitor, myeloid cells ($Mac1^{+}Gr1^{+}$); LMPP, lymphoid-primed multipotent progenitor; LT-HSC, long-term hematopoietic stem cell; Meg, megakaryocyte; MEP, megakaryocyte-erythroid progenitor; NK, natural killer cell; Plas, plasma cell; ST-HSC, short-term hematopoietic stem cell; T_{CD4+}, T helper cell; T_{CD8+}, cytotoxic T cell; T_{reg}, regulatory T cell.

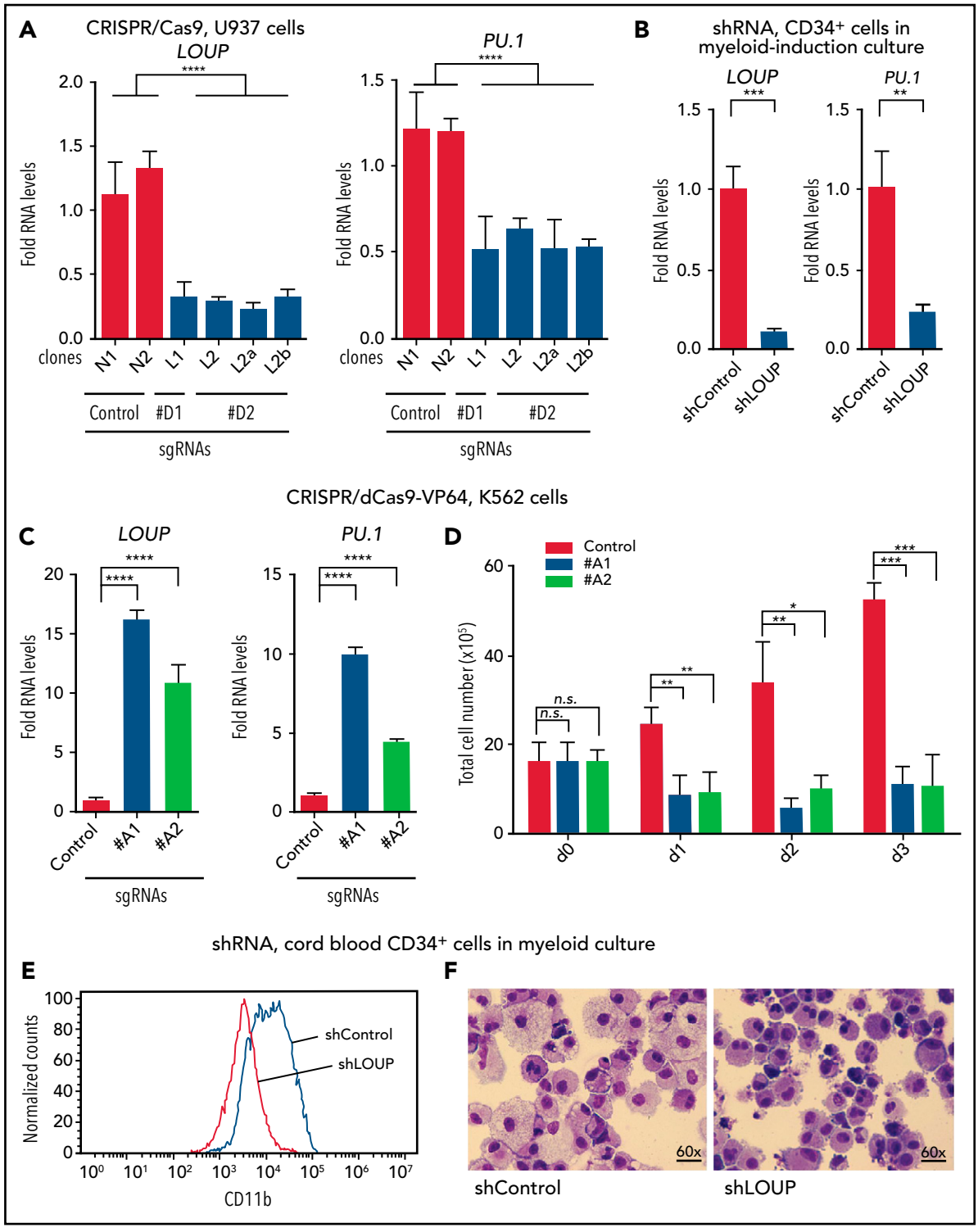

Figure 4. The effect of *LOUP* on *PU.1* expression, myeloid differentiation, and cell growth. (A-C) qRT-PCR expression analysis for *LOUP* (left panels) and *PU.1* (right panels). (A) Nontargeting (N) and *LOUP*-targeting (L) U937 CRISPR/Cas9 cell clones. Data are shown relative to N1 control. (B) Cord blood CD34$^+$ HSPCs stably transfected with *LOUP*-targeting (shLOUP) or nontargeting (shControl) shRNAs by lentiviral transduction and grown in liquid culture with myeloid differentiation-promoting cytokines for 12 days. (C) K562 dCas9-VP64-stable cells infected with *LOUP*-targeting (#A1 and #A2) or nontargeting (Control) sgRNAs. (D) Trypan blue exclusion and manual cell counts for kinetics of cell growth (sgControl *vs* sgLOUP [#A1 and #A2]). (E) Representative flow cytometry results of CD11b myeloid marker expression. Cord blood CD34$^+$ HSPCs stably transfected with either shLOUP shRNA or shControl shRNA by lentiviral transduction and grown in liquid culture with myeloid differentiation-promoting cytokines for 12 days. (F) Camco Stain Pak staining of shControl and shLOUP samples as described in panel E. Representative images were acquired with a Nikon Eclipse microscope (original magnification, ×60) and the SPOT Insight2 camera. Error bars indicate SD (n = 3). $^*P < .05$; $^{**}P < .01$; $^{***}P < .001$; $^{****}P < .0001$. See also supplemental Figure 4 and supplemental Table 3. *n.s.*, not significant.

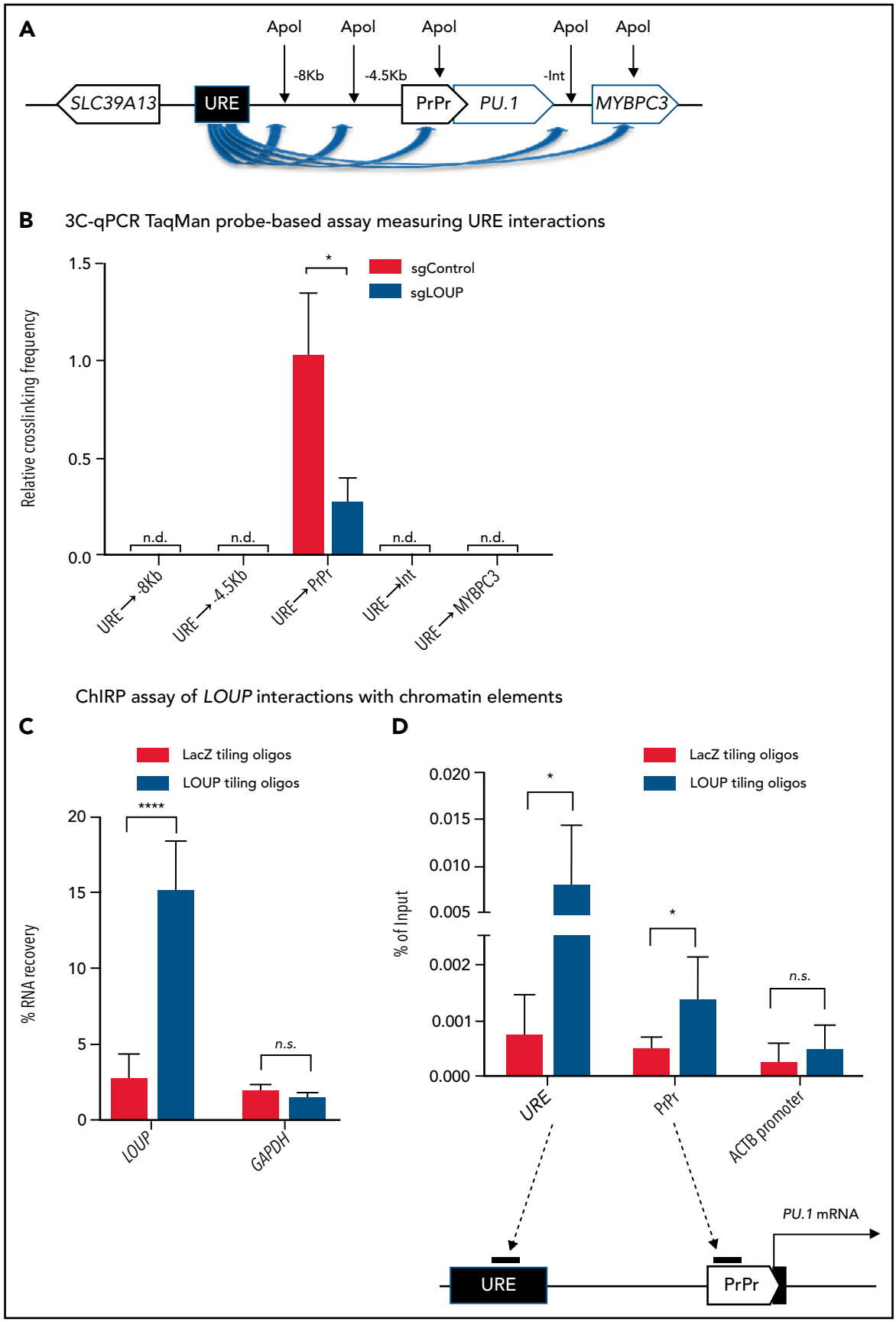

Figure 5. 3C and ChIRP assays measuring the effect of *LOUP* on chromatin looping. (A) Schematic diagram illustrating potential 3C interactions between the URE and genomic viewpoints surrounding the *PU.1* locus. Included are restriction recognition sites of *Apo*I used in the assay. -8 kb and -4 kb are distances from the PrPr in kilobases. (B) 3C-qPCR TaqMan probe-based assay comparing cross-linking frequencies at chromatin viewpoints. The U937 cell clone L2a, carrying a *LOUP*-homozygous indel

(supplemental Figure 4J). Additionally, *LOUP* knockdown in CD34$^+$ HSPCs resulted in cells with less-differentiated morphology and a reduction in the expression level of the macrophage marker *CD14* upon myeloid induction (Figure 4F; supplemental Figure 4K). Together, these results demonstrate that *LOUP* promotes myeloid differentiation and inhibits cell growth.

LOUP induces enhancer-promoter communication by interacting with chromatin at the *PU.1* locus

We have previously reported that the formation of a chromatin loop mediated by URE-PrPr interaction is crucial for *PU.1* induction.[18,19] Because *LOUP* arises from the URE and extends toward the PrPr, we reasoned that *LOUP* drives long-range transcription of *PU.1* by promoting URE-PrPr interaction. To elucidate this, we quantified interaction strengths of the URE with the PrPr and the surrounding area by chromosome conformation capture and TaqMan qPCR (3C-qPCR) (Figure 5A). Consistent with previous reports,[18,19] we detected strong interaction between the URE and the PrPr, but not between the URE and other genomic regions, including the upstream *PU.1* promoter, intergenic sequences, and the *MYBPC3* gene body downstream of the *PU.1* locus. Interestingly, *LOUP* depletion caused a significant reduction in URE-PrPr communication (Figure 5B). To provide evidence supporting our prediction that *LOUP* recruits the URE to the PrPr by physically interacting with the 2 elements, we used the chromatin isolation by RNA purification (ChIRP) assay.[37] Biotinylated *LOUP*-tiling oligos were able to capture endogenous *LOUP* RNA in U937 cells (Figure 5C). Enrichment of the URE and the PrPr cocaptured with *LOUP* RNA was observed in ChIRP-ed samples with *LOUP*-tiling probes but not LacZ-tiling controls, suggesting that *LOUP* occupies both the URE and the PrPr (Figure 5D). Taken together, our data indicate that by interacting and bringing to close proximity 2 regulatory elements, the URE and the PrPr, *LOUP* promotes the formation of a functional chromatin loop within the *PU.1* locus that is critical in inducing *PU.1* expression.

LOUP binds the Runt domain of RUNX1 and coordinates recruitment of RUNX1 to the enhancer and the promoter

Because *LOUP* interacts with RUNX1 (Figure 1), we asked whether *LOUP* mediates the URE-PrPr interaction by cooperating with RUNX1. In line with the previous finding in murine cells,[15] we observed RUNX1 occupancy at the URE in primary CD34$^+$ cells isolated from healthy donors and patients with AML. Importantly, we noticed a peak at the PrPr, indicating that RUNX1 also occupies the PrPr (Figure 6A). We further inspected the genomic region surrounding the PrPr and found a RUNX-DNA–binding consensus motif at -220 bp relative to the *PU.1* mRNA transcription start site. Biotinylated DNA pulldown (DNAP) assays demonstrated that probes, containing the RUNX consensus motifs embedded in the URE and the PrPr, efficiently captured endogenous RUNX1 from U937 nuclear extracts (Figure 6B; supplemental Figure 5A), suggesting that RUNX1 binds its DNA consensus motif at both the URE and the PrPr. Furthermore, our ChIP-qPCR data revealed that RUNX1 occupancy at both the URE and the PrPr was reduced upon *LOUP* depletion (Figure 6C) but increased following *LOUP* induction (supplemental Figure 5B), indicating that *LOUP* promotes placement of RUNX1 dimers at the URE and the PrPr. Besides, *LOUP* depletion was associated with reduced C/EBPα occupancy (supplemental Figure 5C), but had no effect on PU.1 occupancy in the URE (supplemental Figure 5D), suggesting the involvement of *LOUP* in C/EBPα recruitment.

By aligning the *LOUP* sequence with itself using the Basic Local Alignment Search Tool (BLAST), we unexpectedly uncovered a highly repetitive region (RR) of 670 bp near the 3′ end of *LOUP* (supplemental Figure 5E). Interestingly, by performing RNA pulldown (RNAP) assays, we noted that biotinylated *LOUP* RR was able to capture endogenous RUNX1 proteins in U937 nuclear extracts at a level that was comparable to biotinylated full-length *LOUP*, indicating that the RR contains the RUNX1-binding region (Figure 6D; supplemental Figure 5F). To further locate the binding region, we first computed the potential interaction strength of putative elements within the RR to RUNX1 protein by using the catRAPID algorithm.[38] By doing so, we identified 2 ∼100-bp candidate regions, termed region 1 (R1) and region 2 (R2), with high interaction scores (Figure 6E; supplemental Figure 5G). We also identified a repertoire of RIP peaks containing sequences similar to that of R1 or R2, indicating that these regions might represent general RUNX1-binding motifs (supplemental Tables 5 and 6). RNAP analysis confirmed that R1 and R2 bind recombinant RUNX1 (Figure 6F; supplemental Figure 5H). Additionally, the recombinant Runt domain of RUNX1 was able to bind R1 and R2 (Figure 6G; supplemental Figure 5I), suggesting that the Runt domain is responsible for *LOUP* binding. These data together suggest that *LOUP* binds RUNX1 and coordinates deposition of RUNX1 dimers to the URE and the PrPr.

RUNX1-ETO downregulates *LOUP* in t(8;21) AML by inhibiting histone H3 acetylation and reducing chromatin accessibility at the URE

We further examined how the oncogenic fusion protein RUNX1-ETO, derived from t(8;21) chromosomal translocation, affects the regulatory function of *LOUP*. By examining *LOUP* transcript profiles in an AML RNA-seq data set downloaded from The Cancer Genome Atlas (TCGA), we noticed that *LOUP* RNA levels were significantly lower in t(8;21) patients with AML as compared with AML patients with normal karyotype (supplemental Figure 6A left panel). Consistent with our data demonstrating that *PU.1* is a downstream target of *LOUP*, *PU.1* levels were also lower in t(8;21) patients with AML (supplemental Figure 6A right panel). These findings were further confirmed by qRT-PCR using patient samples (Figure 7A). Additionally, we found a robust correlation between *LOUP* and *PU.1* RNA levels (supplemental Figure 6B). Thus, we reasoned that *LOUP* may act as an inhibitory target of RUNX1-ETO in t(8;21) AML. Indeed, RUNX1-ETO overexpression repressed *LOUP* and *PU.1* expression (Figure 7B; supplemental Figure 6C-D). Importantly, enforced *LOUP* expression rescues RUNX1-ETO's effect on *PU.1* inhibition (Figure 7B), indicating *LOUP*-dependent induction of *PU.1*. Conversely, depletion of

Figure 5 (continued) that does not alter the recognition pattern of *ApoI* (supplemental Figure 4D), was used to compare with nontargeting control (sgControl, N1). (C) qRT-PCR assay evaluating levels of *LOUP* RNA and control *GAPDH* captured by biotinylated *LOUP*-tiling and LacZ-tiling probes using ChIRP. (D) ChIRP assay assessing *LOUP* occupancies at the URE, the PrPr, and *ACTB* promoter. LOUP-tiling oligos were used to capture endogenous *LOUP* in U937 cells. LacZ-tiling oligos were used as negative control. Error bars indicate SD (n = 3). $^*P < .05$; $^{****}P < .0001$. Int, intergenic; n.d., not detectable.

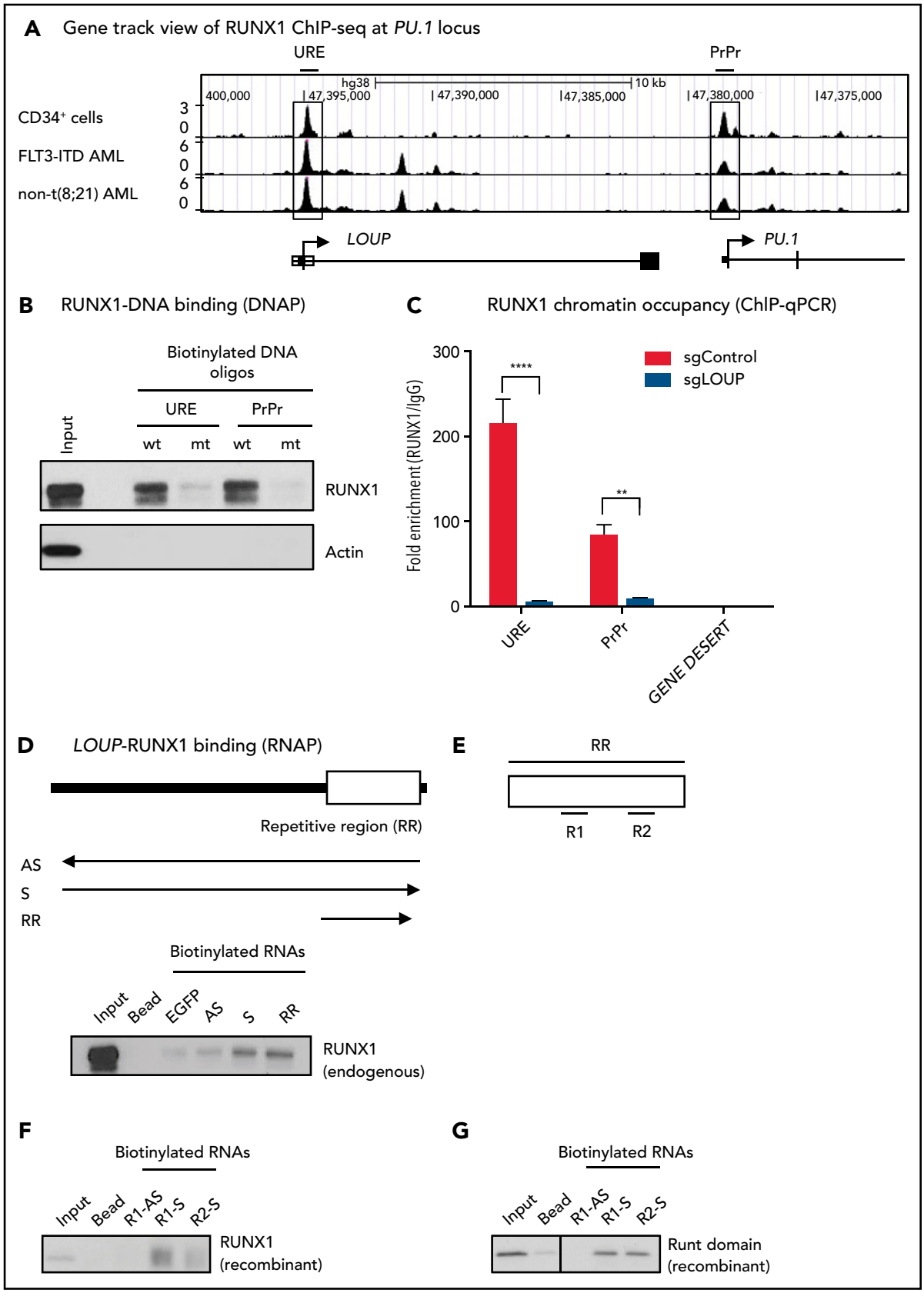

Figure 6. *LOUP* cooperates with RUNX1 to facilitate URE-PrPr interaction. (A) Gene track view of the ~26-kb region encompassing the URE and the PrPr. Top panel: RUNX1 ChIP-seq tracks derived from CD34$^+$ cells from healthy donors (GSM1097884), and a patient with FLT3-ITD AML (GSM1581788). Bottom panel: a schematic showing the corresponding genomic locations of *LOUP* and the 5′ region of *PU.1*. (B) DNA pulldown assay showing binding of RUNX1 to the RUNX1-binding motifs at the URE and the PrPr. Proteins captured by biotinylated DNA oligos (wild-type oligo containing RUNX1-binding motif [wt]; oligo

RUNX1-ETO in t(8;21) AML cell Kasumi-1 by either small interfering RNAs (siRNAs) or shRNAs resulted in a robust increase in *LOUP* transcript levels, accompanied by a significant induction in *PU.1* mRNA (supplemental Figure 6E-F). RUNX1-ETO is capable of recruiting the nuclear receptor corepressor histone deacetylase complex and associates with histone deacetylase activity.[39-41] To examine whether RUNX1-ETO inhibits *LOUP* transcription by affecting local histone acetylation, we analyzed histone acetylation and chromatin accessibility at the URE, where *LOUP* transcription is initiated, upon depletion of RUNX1-ETO.[42] As expected, knockdown of RUNX1-ETO reduces RUNX1-ETO occupancy at the URE (Figure 7C, top panel). Interestingly, depletion of RUNX1-ETO resulted in a robust induction of the H3K9Ac histone acetylation mark (Figure 7C, middle panel; supplemental Figure 6G), and DNase I accessibility at the URE (Figure 7C, bottom panel). We further confirmed that RUNX1-ETO binds the RUNX1 sites in the URE (Figure 7D; supplemental Figure 6H). Taken together, our data indicate that RUNX1-ETO exerts its opposing regulatory effect on *PU.1* expression, at least in part, by inhibiting *LOUP* transcription through reducing URE accessibility.

In summary, we established *LOUP* as a myeloid-specific lncRNA that promotes myeloid differentiation and inhibits cell growth via cooperating with RUNX1 to induce *PU.1* expression, and also established that RUNX1-ETO disrupts the action of *LOUP* in t(8;21) AML. Thus, lncRNA *LOUP* acts as a regulatory hub delivering opposing effects from a broadly expressed transcription factor and its oncogenic derivative on long-range transcription of an important lineage gene (Figure 7E).

Discussion

In this study, we discovered that RUNX1, which is expressed and exerts its regulatory roles in diverse cell types,[43,44] cooperates with myeloid-specific lncRNA *LOUP* to induce long-range transcription of *PU.1*, and that RUNX1-ETO impairs *LOUP*-mediated *PU.1* induction by inhibiting *LOUP* expression in t(8;21) AML. Our study reported several important mechanistic findings. We reveal *LOUP* as a cellular RNA-interacting partner of RUNX1. We also demonstrate that *LOUP* recruits RUNX1 to respective RUNX1-binding motifs at both the URE and the PrPr, thereby promoting formation of the URE-PrPr chromatin loop at the *PU.1* locus. Additionally, we identify a repetitive region serving as the RUNX1-binding platform for *LOUP*. Furthermore, we show that *LOUP* is an inhibitory target of RUNX1-ETO in t(8;21) AML. These findings provide important insight into how long-range transcription is induced in a gene-specific manner by ubiquitous transcription factors and how their chimeric derivatives disrupt normal gene induction in leukemia.

Our findings that RUNX1, known to be crucial for URE-PrPr interaction, occupies both the URE and the PrPr of the *PU.1* locus provide a molecular understanding of locus-specific activation. We propose that once the URE and the PrPr are brought into close proximity, RUNX1 molecules that are parts of separate URE- and PrPr-bound complexes might interact, resulting in the formation of the URE-PrPr (enhancer-promoter) transcriptional activation complex. In supporting this mechanism, RUNX1 sites at enhancers and promoters have been shown to be critical for induction of *CSF2* (encoding GM-CSF), *CD34*, and *CEBPA* (encoding C/EBPα),[45-48] suggesting that RUNX1 could also contribute to specific enhancer-promoter docking at these gene loci. In line with this notion, locus-specific enhancer-promoter interaction could be induced by artificially tethering a transcription factor to a promoter.[49] Our findings, therefore, support a model in which specific and on-target enhancer-promoter interactions are achieved by transcription factors, bound to specific motifs both at the enhancer and the target promoter, which are able to dimerize or multimerize, thereby helping to fuse enhancer and promoter transcriptional complexes together.

How chromatin-bound protein complexes at enhancers and target promoters are brought together in a highly specific manner is still poorly understood. Our findings offer several exciting avenues that might explain how locus-specific induction is accomplished. First, we demonstrated that *LOUP* modulates recruitment of RUNX1 to its binding motifs at both the URE and the PrPr, suggesting that *LOUP* might serve as an "RNA bridge," bringing the separate RUNX1-containing URE and PrPr transcriptional complexes into proximity, which finally fused into an URE-PrPr complex via RUNX1 dimerization. Second, locus specificity might also be enhanced based on our finding that *LOUP* arises from the URE and acts in *cis* to modulate chromatin looping at the nearby *PU.1* locus. Accordingly, even when a small number of transcripts are being produced, local molecular concentration of *LOUP* could be enriched enough to profoundly influence rapid *PU.1* mRNA induction. Indeed, we found that *LOUP* is a low-abundance lncRNA but is enriched in the chromatin fraction. Third, we revealed that *LOUP* is expressed exclusively in myeloid cells. This could explain why RUNX1, which is expressed in diverse cell types, induces URE-PrPr interaction and *PU.1* expression specifically in myeloid cells. These findings, together, provide mechanistic understanding of gene-specific enhancer-promoter interaction and cell type-specific gene induction.

Our findings also contribute to the growing body of knowledge with regard to molecular functions of lncRNAs. Indeed, among thousands of lncRNAs that arise throughout the genomes, only a few have been precisely mapped and molecularly characterized.[23] The herein-described lncRNA *LOUP*, presenting as spliced and polyadenylated transcripts, binds the Runt domain of RUNX1 via a repetitive region. Whether the minor transcript, originating from a splicing event within the second exon of *LOUP*, exhibits other molecular functions remains an open question and is being

Figure 6 (continued) with mutated RUNX1-binding motif [mt]) in U937 nuclear lysate were detected by immunoblot. (C) ChIP-qPCR analysis of RUNX1 occupancy at the URE and the PrPr. *LOUP*-depleted U937 (sgLOUP, L2a) and control (sgControl, N1) clones were used. PCR amplicons include the URE (contains known RUNX1-binding motif at the URE), PrPr (contains putative RUNX1-binding motif in the PrPr), and GENE DESERT (a genome region that is devoid of protein-coding genes). Error bars indicate SD (n = 3). $^{**}P < .01$; $^{****}P < .0001$. (D) RNA pulldown analysis of the RUNX1-*LOUP* interaction. Top panel: schematic diagram of *LOUP* showing the relative position of the repetitive region (RR). Arrows underneath the diagram illustrate direction and relative lengths of in vitro–transcribed and biotin-labeled *LOUP* fragments (AS, full-length antisense control; Bead, no RNA control; EGFP, *EGFP* mRNA control; RR; S, full-length sense). Bottom panel: *LOUP* fragments were incubated with U937 nuclear lysate. Retrieved proteins were identified by immunoblot. (E) Schematic diagram of the repetitive region (RR) showing predicted binding regions R1 and R2. (F-G) RNAP-binding analysis of R1 and R2 with recombinant full-length and Runt domain of RUNX1. In vitro-transcribed and biotin-labeled RNAs include R1-AS (R1 antisense control); R1-S (R1 sense); and R2-S (R2 sense). The vertical line demarcates where an unrelated lane was removed from the figure. See also supplemental Figure 5.

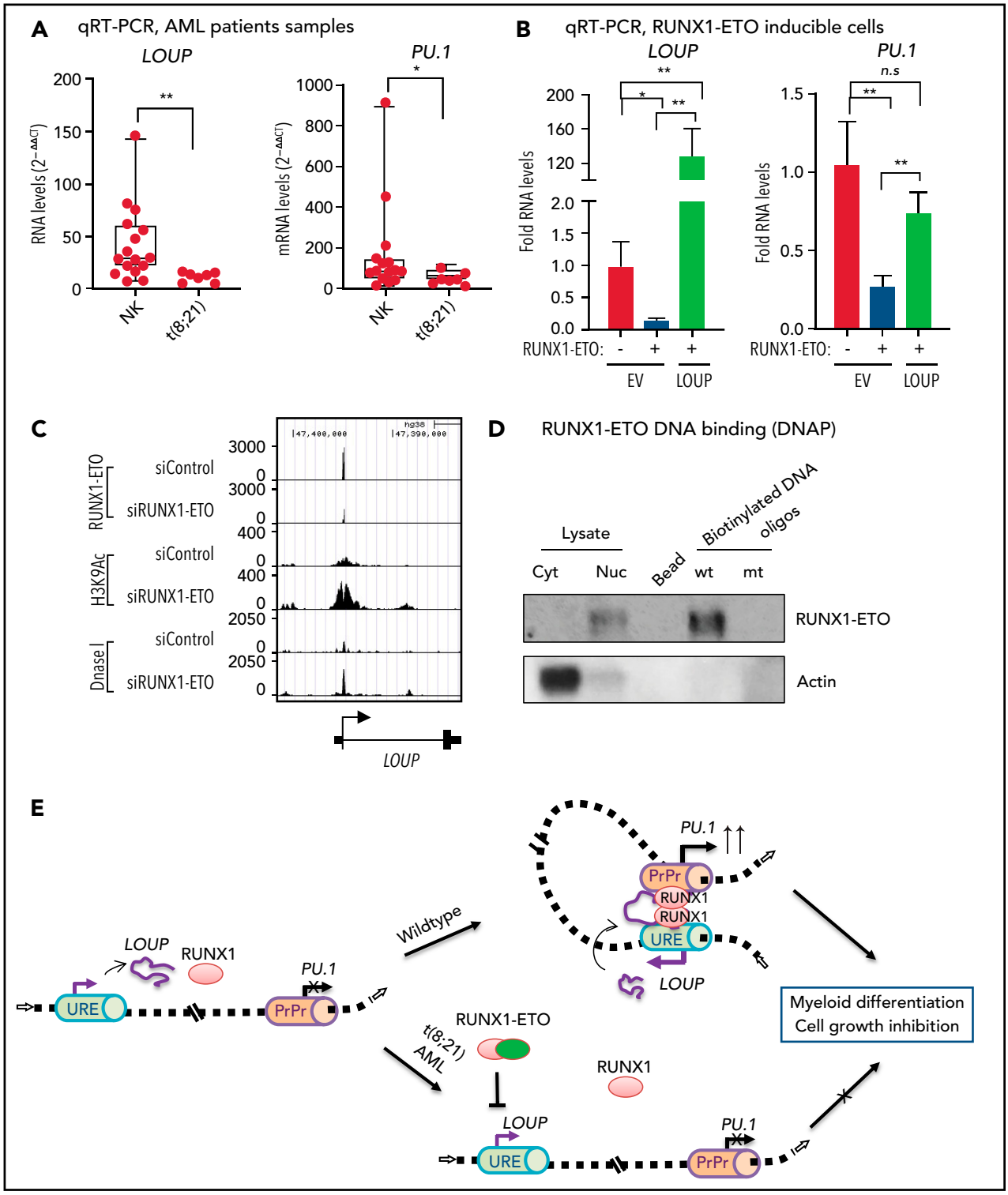

Figure 7. Effects of RUNX1-ETO on regulatory function of *LOUP*. (A) qRT-PCR analysis of samples from patients with AML. Normal karyotype (NK), n = 14; t(8;21) karyotype, n = 7. Mann-Whitney *U* test: $^{**}P < .01$; $^{*}P < .05$. (B) qRT-PCR expression analysis of *LOUP* RNA (left panel) and *PU.1* mRNA (right panel) in U937 cells with inducible expression of RUNX1-ETO (+/−, with/without induction). Cells were transfected with empty vector (EV) and *LOUP* cDNA. Error bars indicate SD (n = 3). $^{*}P < .05$; $^{**}P < .01$. (C) Gene track view at the *LOUP* locus including the URE where *LOUP* transcription initiation is located. From top to bottom are RUNX1-ETO ChIP-seq tracks, H3K9Ac ChIP-seq tracks, and DNase-seq tracks of Kasumi-1 cells upon depletion of RUNX1-ETO. Cells were transfected with either nontargeting siRNA (siControl) or RUNX1-ETO–targeting siRNA. Data were processed from a published data set (GEO GSE29222) and integrated into the UCSC genome browser. (D) DNA pulldown assay showing binding of RUNX1-ETO to the RUNX1-binding motifs at the URE. Proteins captured by biotinylated DNA oligos (wild-type oligo containing RUNX1-binding motif [wt]; oligo with mutated RUNX1-binding motif [mt]) in Kasumi-1 nuclear lysate were detected by immunoblot (cytosol fraction [cyt]; nuclear fraction [nuc]). (E) A model of how *LOUP*

investigated. To our knowledge, *LOUP* is the first cellular RNA-interacting partner of RUNX1 being reported. Remarkably, we also discovered that *LOUP* is downregulated by RUNX1-ETO. It is also worth mentioning that a normal allele of *RUNX1* is retained alongside RUNX1-ETO fusion gene in t(8;21) AML cells,[50] and that RUNX1-ETO is implicated in exerting opposing effects by competing with RUNX1 for binding to protein partners and to RUNX1-binding sites, but not affecting URE-PrPr interaction.[42,51,52] Collectively, our findings uncover heretofore-unknown cross-regulation and molecular interactions of lncRNAs with transcription factors and their oncogenic derivatives, providing mechanistic understanding underlying their molecular functions.

In summary, we identified lncRNA *LOUP* with several important molecular features, including cell type–specific expression and harboring a RUNX1-binding platform enabling *LOUP* to coordinate with RUNX1 to drive long-range transcription of *PU.1* in myeloid cells. *LOUP*, a downstream inhibitory target of the oncogenic fusion protein RUNX1-ETO, is capable of inducing myeloid differentiation and inhibiting cell growth. Our finding raises the possibility that RNA regulators of transcription factors represent alternative targets for therapeutic development and provide a molecular mechanism explaining, at least in part, how ubiquitous transcription factors contribute to enhancer-promoter communication in both a cell type- and a gene-specific manner and how their chimeric derivatives disrupt this normal regulation in leukemia.

Acknowledgments

B.Q.T. thanks Linus Tsai and Touati Benoukraf for technical advice. The authors thank the Iannis Aifantis Laboratory for the generous gift of the sgRNA cloning vector, Robert Welner, To-Ha Thai, and Dong-Er Zhang for insightful comments. The authors also thank Junyan Zhang, Li Ying, Zen Xi, Sophie Kellaway, Qiling Zhou, Georges Lacaud, and Constanze Bonnifer for assistance and helpful suggestions.

This work was supported by the following grants and awards: National Institutes of Health (NIH) National Cancer Institute grants K01 CA222707 (B.Q.T.), R50 CA211304 (A.K.E.), and R00 CA188595 (A.D.R.); an Italian Association for Cancer Research (AIRC) award (A.D.R.); a US Department of Defense (DOD) grant W81XWH-20-1-0518 as well as AIRC awards 5x1000 ("Metastatic disease: the key unmet need in oncology," to the MYNERVA Project), #21267 (M.T.V.); NIH National Heart, Lung, and Blood Institute grant P01HL095489 (L.C.); and an award from the Xiu Research Fund (L.C.). This work was also supported by NIH grants R35 CA197697 (from the National Cancer Institute) and P01HL131477 (from the National Heart, Lung, and Blood Institute), the Singapore Ministry of Health's National Medical Research Council under its Singapore Translational Research (STaR) Investigator Award, the National Research Foundation Singapore, and the Singapore Ministry of Education under its Research Centres of Excellence initiative (D.G.T.).

Authorship

Contribution: B.Q.T. and D.G.T. designed the study with contribution from A.K.E., P.B.S., M.T.V., P.P.P., L.C., S.S.K., and A.D.R.; B.Q.T., S.U., Y.Z., A.K.E., S.C., P.Z., H.Z., E.L., F.M., E.v.d.K., E.F., C.G., and A.R.T. performed experiments; B.Q.T., V.E.A., and G.H. analyzed ChIP-seq data; B.Q.T. and M.A.B. analyzed RIP-seq and scRNA-seq data; B.Q.T. and T.M.N. analyzed bulk RNA-seq data and performed CRISPRa; R.C. and D.E.T. designed and performed RIP-seq experiments; H.Y. and B.Q.T. analyzed TCGA data; C.-S.W. and B.Q.T. performed PhyloCSF analysis; B.Q.T. and S.U. drew schematics; B.Q.T. and D.G.T. wrote the manuscript with input from authors, especially A.K.E., E.L., M.A.B., T.M.N., P.B.S., M.T.V., P.P.P., and A.D.R.; and D.G.T. supervised the project.

Conflict-of-interest disclosure: The authors declare no competing financial interests.

ORCID profiles: B.Q.T., 0000-0002-0956-8941; S.U., 0000-0001-6009-3892; M.A.B., 0000-0003-4322-2968; G.H., 0000-0001-8742-5631; E.F., 0000-0002-6209-8934; C.G., 0000-0001-6829-5544; V.E.A., 0000-0002-3268-8730; A.R.T., 0000-0002-1819-3192; F.M., 0000-0002-7318-9137; E.L., 0000-0003-4612-3105; M.T.V., 0000-0002-6164-4761; L.C., 0000-0003-1937-4750; A.D.R., 0000-0002-9705-4245; D.G.T., 0000-0002-6423-3888.

Correspondence: Daniel G. Tenen, Cancer Science Institute of Singapore, #12-01, MD6, 14 Medical Dr, 117599 Singapore; e-mail: daniel.tenen@nus.edu.sg; and Bon Q. Trinh, Harvard Medical School Innitiative for RNA Medicines, Center for Life Sciences, 3 Blackfan Circle, Boston, MA 02215; e-mail: btrinh@bidmc.harvard.edu.

Footnotes

Submitted 29 June 2020; accepted 18 April 2021; prepublished online on *Blood* First Edition 10 May 2021. DOI 10.1182/blood.2020007920.

The sequencing data reported in this article have been deposited in the Gene Expression Omnibus database (accession number GSE140459 [https://www.ncbi.nlm.nih.gov/geo/query/acc.cgi?acc=GSE140459; enter token evstyyqkznmvtox]).

The online version of this article contains a data supplement.

There is a *Blood* Commentary on this article in this issue.

The publication costs of this article were defrayed in part by page charge payment. Therefore, and solely to indicate this fact, this article is hereby marked "advertisement" in accordance with 18 USC section 1734.

REFERENCES

1. Shivdasani RA, Orkin SH. The transcriptional control of hematopoiesis. *Blood*. 1996;87(10):4025-4039.
2. Novershtern N, Subramanian A, Lawton LN, et al. Densely interconnected transcriptional circuits control cell states in human hematopoiesis. *Cell*. 2011;144(2):296-309.
3. Iwasaki H, Mizuno S, Arinobu Y, et al. The order of expression of transcription factors directs hierarchical specification of hematopoietic lineages. *Genes Dev*. 2006;20(21):3010-3021.
4. Tenen DG, Hromas R, Licht JD, Zhang DE. Transcription factors, normal myeloid development, and leukemia. *Blood*. 1997;90(2):489-519.
5. Chen HM, Zhang P, Voso MT, et al. Neutrophils and monocytes express high levels of PU.1 (Spi-1) but not Spi-B. *Blood*. 1995;85(10):2918-2928.
6. Rosenbauer F, Wagner K, Kutok JL, et al. Acute myeloid leukemia induced by graded reduction of a lineage-specific transcription factor, PU.1. *Nat Genet*. 2004;36(6):624-630.
7. Cook WD, McCaw BJ, Herring C, et al. PU.1 is a suppressor of myeloid leukemia, inactivated in mice by gene deletion and mutation of its DNA binding domain. *Blood*. 2004;104(12):3437-3444.
8. Huang G, Zhang P, Hirai H, et al. PU.1 is a major downstream target of AML1 (RUNX1) in adult mouse hematopoiesis [published correction appears in *Nat Genet*. 2008;40(2):255]. *Nat Genet*. 2008;40(1):51-60.
9. Chen CL, Broom DC, Liu Y, et al. Runx1 determines nociceptive sensory neuron phenotype and is required for thermal and neuropathic pain. *Neuron*. 2006;49(3):365-377.
10. Hoi CS, Lee SE, Lu SY, et al. Runx1 directly promotes proliferation of hair follicle stem cells and epithelial tumor formation in mouse skin. *Mol Cell Biol*. 2010;30(10):2518-2536.

11. Osorio KM, Lilja KC, Tumbar T. Runx1 modulates adult hair follicle stem cell emergence and maintenance from distinct embryonic skin compartments. *J Cell Biol*. 2011;193(1):235-250.

12. North TE, de Bruijn MF, Stacy T, et al. Runx1 expression marks long-term repopulating hematopoietic stem cells in the midgestation mouse embryo. *Immunity*. 2002;16(5): 661-672.

13. Miyoshi H, Shimizu K, Kozu T, Maseki N, Kaneko Y, Ohki M. t(8;21) breakpoints on chromosome 21 in acute myeloid leukemia are clustered within a limited region of a single gene, AML1. *Proc Natl Acad Sci USA*. 1991;88(23):10431-10434.

14. Erickson P, Gao J, Chang KS, et al. Identification of breakpoints in t(8;21) acute myelogenous leukemia and isolation of a fusion transcript, AML1/ETO, with similarity to Drosophila segmentation gene, runt. *Blood*. 1992;80(7):1825-1831.

15. Staber PB, Zhang P, Ye M, et al. The Runx-PU.1 pathway preserves normal and AML/ETO9a leukemic stem cells. *Blood*. 2014; 124(15):2391-2399.

16. Bulger M, Groudine M. Functional and mechanistic diversity of distal transcription enhancers. *Cell*. 2011;144(3):327-339.

17. Levine M. Transcriptional enhancers in animal development and evolution. *Curr Biol*. 2010; 20(17):R754-R763.

18. Ebralidze AK, Guibal FC, Steidl U, et al. PU.1 expression is modulated by the balance of functional sense and antisense RNAs regulated by a shared cis-regulatory element. *Genes Dev*. 2008;22(15):2085-2092.

19. Staber PB, Zhang P, Ye M, et al. Sustained PU.1 levels balance cell-cycle regulators to prevent exhaustion of adult hematopoietic stem cells. *Mol Cell*. 2013;49(5):934-946.

20. Li Y, Okuno Y, Zhang P, et al. Regulation of the PU.1 gene by distal elements. *Blood*. 2001; 98(10):2958-2965.

21. Djebali S, Davis CA, Merkel A, et al. Landscape of transcription in human cells. *Nature*. 2012;489(7414):101-108.

22. Ponting CP, Oliver PL, Reik W. Evolution and functions of long noncoding RNAs. *Cell*. 2009;136(4):629-641.

23. Uszczynska-Ratajczak B, Lagarde J, Frankish A, Guigó R, Johnson R. Towards a complete map of the human long non-coding RNA transcriptome. *Nat Rev Genet*. 2018;19(9): 535-548.

24. Mercer TR, Dinger ME, Mattick JS. Long non-coding RNAs: insights into functions. *Nat Rev Genet*. 2009;10(3):155-159.

25. Rinn JL, Chang HY. Genome regulation by long noncoding RNAs. *Annu Rev Biochem*. 2012;81:145-166.

26. Di Ruscio A, Ebralidze AK, Benoukraf T, et al. DNMT1-interacting RNAs block gene-specific DNA methylation. *Nature*. 2013;503(7476): 371-376.

27. Arber DA, Orazi A, Hasserjian R, et al. The 2016 revision to the World Health Organization classification of myeloid neoplasms and acute leukemia [published correction appears in Blood. 2016;128(3):462–463]. *Blood*. 2016;127 (20):2391-2405.

28. Hendrickson DG, Kelley DR, Tenen D, Bernstein B, Rinn JL. Widespread RNA binding by chromatin-associated proteins. *Genome Biol*. 2016;17:28.

29. Zhao J, Ohsumi TK, Kung JT, et al. Genome-wide identification of polycomb-associated RNAs by RIP-seq. *Mol Cell*. 2010;40(6):939-953.

30. Hunt SE, McLaren W, Gil L, et al. Ensembl variation resources. *Database (Oxford)*. 2018; 2018:bay119.

31. Creyghton MP, Cheng AW, Welstead GG, et al. Histone H3K27ac separates active from poised enhancers and predicts developmental state. *Proc Natl Acad Sci USA*. 2010;107(50): 21931-21936.

32. Pekowska A, Benoukraf T, Zacarias-Cabeza J, et al. H3K4 tri-methylation provides an epigenetic signature of active enhancers. *EMBO J*. 2011;30(20):4198-4210.

33. Lin MF, Jungreis I, Kellis M. PhyloCSF: a comparative genomics method to distinguish protein coding and non-coding regions. *Bioinformatics*. 2011;27(13):i275-i282.

34. Finn RD, Coggill P, Eberhardt RY, et al. The Pfam protein families database: towards a more sustainable future. *Nucleic Acids Res*. 2016;44(D1):D279-D285.

35. Tenen DG. Disruption of differentiation in human cancer: AML shows the way. *Nat Rev Cancer*. 2003;3(2):89-101.

36. DeKoter RP, Singh H. Regulation of B lymphocyte and macrophage development by graded expression of PU.1. *Science*. 2000; 288(5470):1439-1441.

37. Chu C, Quinn J, Chang HY. Chromatin isolation by RNA purification (ChIRP). *J Vis Exp*. 2012;(61):3912.

38. Bellucci M, Agostini F, Masin M, Tartaglia GG. Predicting protein associations with long noncoding RNAs. *Nat Methods*. 2011;8(6): 444-445.

39. Gelmetti V, Zhang J, Fanelli M, Minucci S, Pelicci PG, Lazar MA. Aberrant recruitment of the nuclear receptor corepressor-histone deacetylase complex by the acute myeloid leukemia fusion partner ETO. *Mol Cell Biol*. 1998;18(12):7185-7191.

40. Lutterbach B, Westendorf JJ, Linggi B, et al. ETO, a target of t(8;21) in acute leukemia, interacts with the N-CoR and mSin3 corepressors. *Mol Cell Biol*. 1998;18(12):7176-7184.

41. Wang J, Hoshino T, Redner RL, Kajigaya S, Liu JM. ETO, fusion partner in t(8;21) acute myeloid leukemia, represses transcription by interaction with the human N-CoR/mSin3/HDAC1 complex. *Proc Natl Acad Sci USA*. 1998;95(18):10860-10865.

42. Ptasinska A, Assi SA, Mannari D, et al. Depletion of RUNX1/ETO in t(8;21) AML cells leads to genome-wide changes in chromatin structure and transcription factor binding. *Leukemia*. 2012;26(8):1829-1841.

43. Hong D, Fritz AJ, Gordon JA, et al. RUNX1-dependent mechanisms in biological control and dysregulation in cancer. *J Cell Physiol*. 2019;234(6):8597-8609.

44. Deltcheva E, Nimmo R. RUNX transcription factors at the interface of stem cells and cancer. *Biochem J*. 2017;474(11):1755-1768.

45. Cockerill PN, Osborne CS, Bert AG, Grotto RJ. Regulation of GM-CSF gene transcription by core-binding factor. *Cell Growth Differ*. 1996;7(7):917-922.

46. Bowers SR, Calero-Nieto FJ, Valeaux S, Fernandez-Fuentes N, Cockerill PN. Runx1 binds as a dimeric complex to overlapping Runx1 sites within a palindromic element in the human GM-CSF enhancer. *Nucleic Acids Res*. 2010;38(18):6124-6134.

47. Guo H, Ma O, Speck NA, Friedman AD. Runx1 deletion or dominant inhibition reduces Cebpa transcription via conserved promoter and distal enhancer sites to favor monopoiesis over granulopoiesis. *Blood*. 2012;119(19):4408-4418.

48. Levantini E, Lee S, Radomska HS, et al. RUNX1 regulates the CD34 gene in haematopoietic stem cells by mediating interactions with a distal regulatory element. *EMBO J*. 2011;30(19):4059-4070.

49. Deng W, Lee J, Wang H, et al. Controlling long-range genomic interactions at a native locus by targeted tethering of a looping factor. *Cell*. 2012;149(6):1233-1244.

50. Ben-Ami O, Friedman D, Leshkowitz D, et al. Addiction of t(8;21) and inv(16) acute myeloid leukemia to native RUNX1. *Cell Rep*. 2013; 4(6):1131-1143.

51. Loke J, Assi SA, Imperato MR, et al. RUNX1-ETO and RUNX1-EVI1 differentially reprogram the chromatin landscape in t(8;21) and t(3;21) AML. *Cell Rep*. 2017;19(8):1654-1668.

52. Meyers S, Downing JR, Hiebert SW. Identification of AML-1 and the (8;21) translocation protein (AML-1/ETO) as sequence-specific DNA-binding proteins: the runt homology domain is required for DNA binding and protein-protein interactions. *Mol Cell Biol*. 1993;13(10):6336-6345.

53. Prange KHM, Mandoli A, Kuznetsova T, et al. MLL-AF9 and MLL-AF4 oncofusion proteins bind a distinct enhancer repertoire and target the RUNX1 program in 11q23 acute myeloid leukemia. *Oncogene*. 2017;36(23):3346-3356.

54. Zheng GX, Terry JM, Belgrader P, et al. Massively parallel digital transcriptional profiling of single cells. *Nat Commun*. 2017; 8:14049.